Coupled Precipitation-Streamflow Simulations at the GAME/HUBEX Site: Xixian Basin

By Norman L. Miller, Jinwon Kim

Regional Climate Center, Lawrence Berkeley National Laboratory, Berkeley, California, USA

Jian Yun Zhang

Water Resources Information Center, Ministry of Water Resources, Beijing, P.R. China

and

Jai-Ho Oh

Meteorological Research Institute, Korean Meteorological Administration, Seoul, South Korea

(Manuscript received 13 October 1999, in revised form 14 May 2001)

Abstract

As a contribution to the GAME/HUBEX program, we used historical data and the Regional Climate System Model (RCSM) to analyze and simulate precipitation and streamflow in the Xixian basin. Historical data for the period 1982 to 1988 indicates that peak precipitation and streamflow occurs during the summer and early fall, when this region is affected by the East Asian summer monsoons and typhoons, respectively. In preparation for long-term coupled atmospheric and streamflow model simulations, we calibrated the RCSM's semi-distributed hydrologic model (TOPMODEL) for the Xixian basin using observations from 1982 to 1984 and validated for the period 1985 to 1988 with good results.

Long-term hydroclimate simulations generated for the period January 1979 to December 1983 using the RCSM captured important hydroclimate characteristics of the region. The simulated seasonal precipitation and streamflow variations agree well with observations during late fall to spring. Summertime precipitation and streamflow were overestimated in the hindcast. The over-estimated precipitation may be due to the input large-scale forcing and the difficulty in simulating convective precipitation during the monsoon season using a mesoscale atmospheric model. Coupled modeling of regional climate and streamflow is a relatively new capability. Implementation of this technique to river basins in the East Asia region will result in an increased predictability of water resources for this region.

1. Introduction

Understanding the hydrologic response to climate variability and climate change has become a growing international concern. The Global Energy and Water Cycle Experiments (GEWEX) have organized a number of field campaigns to better understand hydrologic response over large regions and at important river basins. The GEWEX Asian Monsoon Experiment (GAME) regions are located in Siberia, the Tibetan Plateau, Indochina, and eastern China, including the Huaihe basin. The GAME/Huaihe Basin Experiment (HUBEX) targets a tributary of the Yangtze River that affects heavily populated industrial and agricultural cen-

Corresponding author: Norman L. Miller, MS90–1116, University of California, Lawrence Berkeley National Laboratory, 1 Cyclotron Road, CA94720, USA.
E-mail: nlmiller@lbl.gov

ters in eastern China.

Coupled limited-area atmospheric and streamflow modeling (Leavseley et al. 1992; Miller and Kim 1996; Leung et al. 1996; Leung et al. 1999; Kim et al. 1998a; Yu et al. 1999) has become an important tool for dynamically downscaling coarse-resolution data to simulate local hydrometeorology for assessing regional climate and its impact on streamflow. Dynamic downscaling systems have successfully been used for short-term predictions of flood events (Miller and Kim 1996; Yu et al. 1999), seasonal hydroclimate predictions (Kim et al. 1998a, 2000a, b; Miller et al. 1999), and analysis of the effects of snow budget on streamflow in mountainous basins (Leavesley et al. 1992; Leung et al. 1996; Kim et al. 1998a). These studies have shown that coupled limited area atmosphere models and streamflow models can capture quantitative precipitation and streamflow for temporal scales from multi-storm events to a season. Such a capability is important for flood forecasting, improved reservoir operation, and water resources assessment.

A focus of the numerical hindcast study presented here is to evaluate the Regional Climate System Model (RCSM) for simulating important hydroclimate features in East Asia. This is important for a better understanding of the magnitude of long-term streamflow response, and how this impacts water resources and agricultural productivity. These hindcast evaluations are a step toward improved simulations of downscaled hydroclimate projections and impact analysis. By diagnosing coupled hindcast simulations, one can move forward with fully coupled streamflow predictions and crop simulations at seasonal time scales with increased confidence. It should be noted that flood modeling requires numerical weather predictions at fine spatial scales for capturing the sub-daily response. This paper focuses on the hydrologic calibration and response at a single basin, and addresses the monthly time scale hindcast as an evaluation of precipitation and streamflow in preparation for a more comprehensive long-term hydroclimate impact assessment that will include a number of additional basins.

The following sections provide a brief summary of the geography and hydroclimatology of the HUBEX area, and an overview of the RCSM. It is followed by discussions of the streamflow model calibration and verification, and results from a downscaled hydroclimate simulation for the HUBEX Xixian basin during the period January 1979 to December 1983.

2. GAME/HUBEX site

The Huaihe is a tributary of the Yangtze River, and is located between 113°E, 31°N and 121°E, 36°N, with a drainage basin area of 185,000 km^2. The Xixian basin (Fig. 1), one of the GAME/HUBEX intensive study sites, is located in the southwestern headwater region of the Huaihe basin with an area of 10,137 km^2. Fig. 2 indicates the locations of the streamflow gauges, rain gauges, and sub-basins within the Xixian basin.

The Xixian basin has low depressed landforms and contains clayey .alluvial-lacustrine deposits (FAO–UNESCO, 1978). The terrain elevation ranges from 15 m above mean sea level at the city of Xixian (streamflow gauge 51012) to over 1,000 m above mean sea level in the western and southern Tongbai and Dabie Mountains (Fig. 2). The flat valley region downstream of the streamflow gage 51010 has an elevation of 15–60 m above mean sea level and is frequently flooded during the summer and fall seasons. Due to limited data, we were unable to obtain natural flows for the entire Xixian basin and have focused on a headwater region. We have selected the basin upstream of the 51010 streamflow gauge in Fig. 2 for this study, since no reservoir controls the streamflow at this location and the discharge from this headwater region significantly affects the city of Xixian and the crops in the valley regions during the wet season. For clarification, the sub-basin that is upstream of stream gauge 51010 will be referred to here as the Xixian study basin.

Mean annual precipitation at four rain gauge stations (51000, 51001, 51005, and 51010), in the Xixian study basin (Table 1) show a strong spatial variation, perhaps due to the orographic forcing by local terrain. The basin-average (arithmetic) mean annual precipitation is 987 mm/year for the ten-year observation period, 1979 to 1988. Despite the strong spatial variation, there were no observed systematic variations as a function of elevation. Investigation of both streamflow and rain gauge records show that storm events exceeding 40 mm/day tends to cause overland flooding. This also depends on the storm frequency and the antecedent soil moisture conditions.

The observed mean-seasonal precipitation at each station is presented in Table 2. The summer (JJA) precipitation was 36.6%, 48.4%, 45.7%, and 45.9%

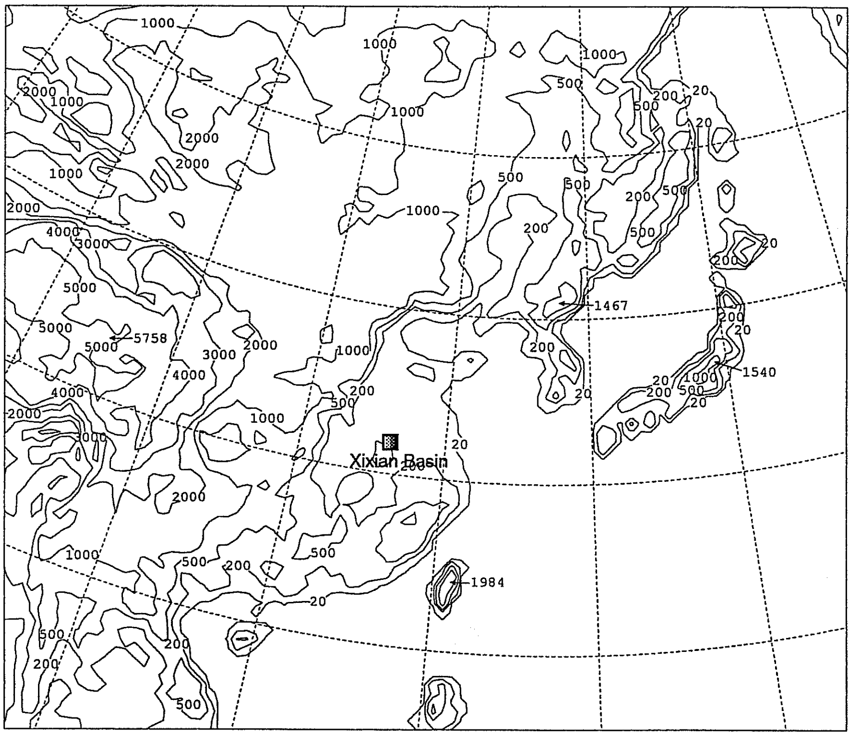

Fig. 1. The East Asian domain used in the RCSM mesoscale simulations and the location of the HUBEX/Xixian study region. Contours (meters) represent the mesoscale topography.

Table 1. Mean annual precipitation within the Xixian study basin.

Station Number	Station Elevation	Annual Precipitation
51000	154 m	1148 mm/year
51001	161 m	844 mm/year
51005	119 m	932 mm/year
51010	58 m	1024 mm/year

Table 2. Mean seasonal precipitation within the Xixian study basin.

Station Number	Winter (DJF)	Spring (MAM)	Summer (JJA)	Fall (SON)
51000	76 mm/season	247 mm/season	532 mm/season	303 mm/season
51001	41 mm/season	177 mm/season	409 mm/season	218 mm/season
51005	60 mm/season	208 mm/season	427 mm/season	240 mm/season
51010	75 mm/season	226 mm/season	472 mm/season	254 mm/season

Table 3. Number of storm events where storm-total precipitation exceeds 40 mm/day.

Station Number	Winter (DJF)	Spring (MAM)	Summer (JJA)	Fall (SON)
51000	0	6	25	13
51001	0	4	10	4
51005	0	4	17	9
51010	0	5	28	12

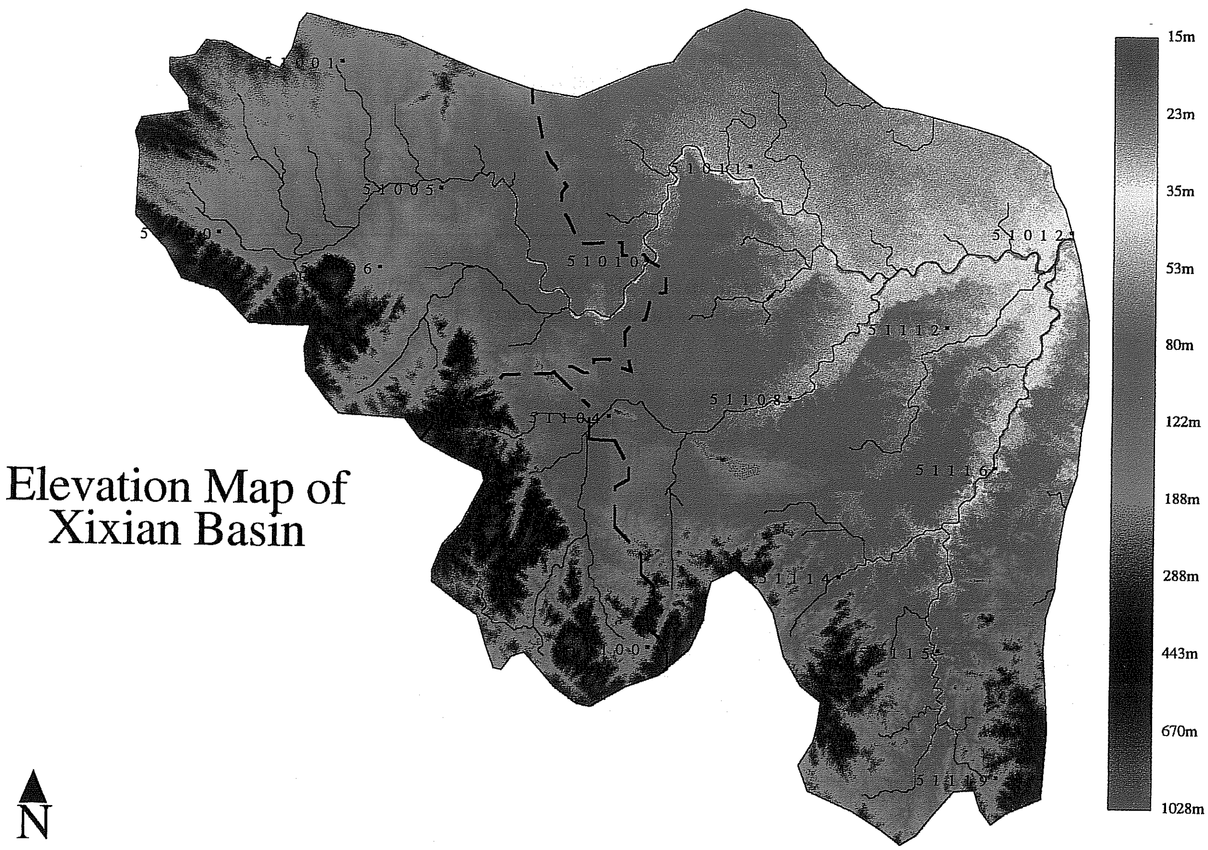

Fig. 2. The Xixian basin, topography, rain gauges, and stream gauges. The Xixian study basin boundary is shown as a dashed line above stream gauge 51010.

of the annual total precipitation at rain gauges 51000, 51001, 51005, and 51010, respectively, with a spatial mean of 46.6%. The spring (MAM) and fall (SON) also received significant precipitation with spatial mean values of 21.7% and 25.7%, respectively, while the winter (DJF) received the least (6%). The majority of the heavy precipitation events occur during the summer season (Table 3), when this region is affected by the summer monsoon. Heavy precipitation is also associated with typhoons that mostly occur during the fall months in this region.

Observed mean-daily streamflow at gage 51010 (Fig. 3) indicates that high streamflow levels occur during July to October and low streamflow is from October to April. Inter-annual variations indicate that 1980, 1981, 1982, and 1987 were above average (periods with streamflow greater than 1000 CMS), while 1985 and 1986 were well below average (less than 500 CMS). For climate analysis purposes, streamflow per basin area with units of mm/day is used (units conversion for the 2,861 km^2 Xixian study basin: 1 CMS = 0.0302 mm/day). The mean annual streamflow at 51010 is 1.01 mm/day (33.4 CMS). The mean seasonal streamflow is; 0.27 mm/day (8.9 CMS) for DJF, 0.55 mm/day (18.2 CMS) for MAM, 1.90 mm/day (62.9 CMS) for JJA, and 1.31 mm/day (43.5 CMS) for SON. It should be noted that 1980, 1982, and 1987 were El Niño years, while 1985 and 1986 were mostly in the La Nina phase. There may be a weak correlation between the El Niño phase of the Southern Oscillation Index and high streamflow. However, the available observed records were too short for this analysis of long-term climate variability to be statistically significant, and other large scale forcing is likely contributing to the streamflow signature, for example, the western Pacific subtropical high (Wang et al. 2000).

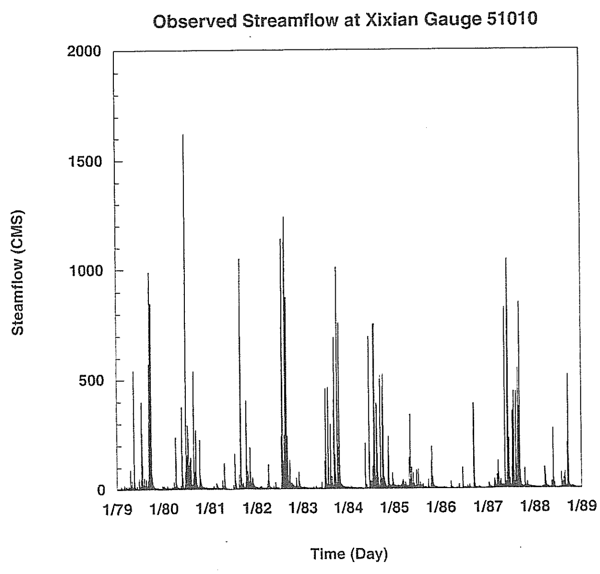

Fig. 3. Observed ten year (1979 to 1988) daily streamflow at the Xixian 51010 gauge.

3. Model description

The Regional Climate System Model (RCSM) is composed of pre- and post-processors and a suite of physically based models. It has been successfully used for weather and climate predictions since 1995 (Miller and Kim 1996; Miller et al. 1996; Miller and Kim 1997; Kim et al. 1998a, b; Miller et al. 1999; Kim et al. 2000). The Mesoscale Atmospheric Simulation (MAS) model (Kim and Soong 1996; Soong and Kim 1996) and Soil-Plant-Snow (SPS) model (Kim and Ek 1995) are interactively coupled (Kim et al. 1998b). MAS–SPS utilizes large-scale data from analysis and GCM simulations to drive the initial and lateral boundary conditions. Output from the MAS–SPS directly drives a suite of one-directionally coupled hydrologic models (lumped, semi-distributed, distributed).

The Mesoscale Atmospheric Simulation (MAS) model is a primitive equation, limited area model with 18 vertical σ-coordinate layers, and a 60 km × 60 km horizontal grid resolution (5400 km × 4800 km) covering East Asia (Fig. 1). The MAS model computes grid-scale condensation and precipitation with a four-class version of the bulk cloud micophysics scheme (Cho et al. 1989). Radiative transfer is based on Harshvardahn et al. (1987) with ice-phase (Stephens et al. 1978) and water-phase (Starr and Cox 1985) cloud particles. MAS includes boundary layer bulk aerodynamics (Deardorff 1978), eddy diffusivities (Louis et al. 1981), and advection (Takacks 1985). The MAS model includes the National Centers for Environmental Prediction (NCEP) cumulus convection scheme (Pan and Wu 1995; Hong and Pan 1998). The two-layer land surface Soil-Plant-Snow (SPS) model (Mahrt and Pan 1984; Kim and Ek 1995) predicts volumetric soil moisture, soil temperature, canopy water content, and water equivalent snow depth. In this study, the coupled MAS–SPS produces the input forcing for the one-directional coupled streamflow simulation, TOPMODEL (Beven and Kirkby 1979).

TOPMODEL may be viewed as a system of vertical reservoirs (interception zone storage, unsaturated infiltration zone storage, and saturated zone storage) formulated using Darcy's Law and water mass continuity. Soil moisture accounting and lateral transport in TOPMODEL are based on two assumptions: (1) the saturated zone dynamics are approximated by successive steady state representations and (2) the hydraulic gradient of the saturated zone is parallel to the surface topography. An important feature of TOPMODEL is the semi-distributed parameterizations and similarity in topographic control of surface and subsurface flows that help to reduce the number of model parameters required for calibration, while maintaining physical representations of the dynamics. The effective depth of available water storage in a soil column is defined here as a saturation storage deficit (SSD), and when this value is less than or equal to zero, then the soil column is saturated and overland flow occurs (Beven et al. 1995).

The version of TOPMODEL used in this study has been modified and configured within the RCSM framework (Miller and Kim 1996). The RCSM version of TOPMODEL includes a power function for the subsurface transmissivity profile (Duan and Miller 1997) and a leakage parameterization. The distribution of the topographic index, λ, is one of the mechanisms for the surface following lateral subsurface transport assumption. Stream channel flow (Q) is defined as the sum of surface flow (Q_s) and subsurface base flow (Q_b), where surface flow consists of two terms, direct overland flow (Hortonian or saturated overland) and return flow associated with the water table reaching the surface. Base flow is defined here as the percent (D) of subsurface water that is laterally transported downslope toward the stream channel, where the percent (1–D) represents the amount lost or leaked to a deep storage zone. Under the assumption that TOPMODEL sequentially fills the saturated zone storage and then the infiltration zone storage, a local storage deficit or effective depth to the water table is determined. Once the local storage deficit reaches zero, there is local saturation and overland flow. Antecedent conditions and surface permeability also determine the rate of infiltration and flow. Due to the limited available data, evapotranspiration is calculated as a function of the day length and temperature (Hamon 1961).

Mesoscale simulations mapped onto a mean area-weighted domain representative of the Xixian study basin are simulated as spatially uniform input to TOPMODEL. This coupling provides the downscale link between GCMs or global reanalysis fields and the watershed scale. In this simulation, neighboring mesoscale grid point values were used to generate mean area forcing variables to TOPMODEL using an area matching method (Kim et al. 2000b). The 60 km mesoscale model resolution allows for initial evaluation of a coupled precipitation-streamflow simulation, however, further nesting (e.g., 10 km) is necessary to capture the details of the local orographic forcing. The following section provides details to the calibration and verification of TOPMODEL at the 51010 stream gauge.

4. TOPMODEL calibration and verification

TOPMODEL calibration consists of two parts, (1) computation of the direct parameters and (2) optimization of the non-directly computable parameters. The direct parameters include latitude, watershed area, soil depths, and the topographic index values (mean, variance, and skewness).

The latitude (32.5°), which is used for the evapotranspiration parameterization (Hamon 1961) during calibration, was determined as the Xixian study basin mean latitude. Soil depths (upper layer equal to 45 cm, total depth equal to 120 cm) were based on the correlated Soil Map of China description of the Huaihe region with the FAO–UNESCO Soil Map of the World (1978). The depth of the root zone (Z_{root}) was set to 40 cm based on the rooting depth of winter wheat and summer rice (L. Mearns, personal communication). The topographic index, $\lambda = a/\tan\beta$, a flow similarity parameter used in the semi-distributed hydrologic model simulation, is the ratio of the upstream flow area, a, that crosses a pixel with slope $\tan\beta$. The topographic index is solved numerically using terrain elevation data and GIS tools (Band 1986; Miller 1997). The Chinese Ministry of Water Resources (MWR) Digital Elevation Model (DEM) data was augmented with the Satellite based 3-arc-sec Digital Terrain Elevation Data Level II (DTED II). Upon merging the MWR DEM and DTED II data, pits and small depressions were removed, pixel flow paths computed, a topographic streamflow network defined, and a topographic index was generated for each 3-arc-sec pixel. The topographic index computed for this region has a mean value of 13.08, variance of

2.02, and skewness of 1.76. This unusually high mean topographic index is due in part to the flat flood plain region with elevation changes of order 30 m, and the steep southwestern mountains (Tongbai and Dabie) with elevations exceeding 1,000 m within approximately 30 km.

Parameters that are not directly determined from the data are calibrated to historical precipitation and streamflow time series, as well as land surface characterizations (topography, vegetation, soil type, depth to bedrock). Parameters that are calibrated in this study are the saturated hydraulic conductivity (K), a scaling parameter describing the decrease in subsurface transmissivity with depth (m), the field capacity (θ), and a leakage parameter (1–D).

Calibration and verification at stream gauge 51010 utilized the observed daily precipitation and streamflow time series corresponding to the Xixian study basin (2,861 km^2). The streamflow model calibration was based on precipitation data derived from the arithmetic mean time series. Once calibration is complete, parameter verification for a different time period of the observational record is performed.

The four calibration parameters (m, D, K, θ) are solved via a two-step optimization procedure. Determination of the best range of values for the parameter set ($j = 1,4$) is based on a Monte Carlo simulation of TOPMODEL about a minimum and maximum range,

$$\begin{aligned}\mathrm{PAR_j} &= \mathrm{PAR_{j,min}} \\ &\quad + \mathrm{random}(\mathrm{PAR_{j,max}} - \mathrm{PAR_{j,min}}), \\ &\quad 0 \le \mathrm{random} \le 1. \end{aligned} \tag{1}$$

Each parameter minimum and maximum initial value was determined by information from similar studies and available basin data (e.g., K was set to 20,000 mm/day and is in the range of values representative of tilled clayey soils). The range for each parameter is narrowed by a Monte Carlo simulation of 1,000 iterations, followed by a second 1,000-iteration simulation with new minimum and maximum values based on the statistical analysis of the upper percentile of model efficiency (Nash and Sutcliffe 1970),

$$\mathrm{Eff} = (1 - \sigma_e/\sigma_o)^n, \tag{2}$$

where σ_e is the variance of residuals, σ_o is the variance of observations, and n is one. Optimized values are determined from the multi-parameter space where the parameter-dependent efficiency is contained over a broad region ($\delta PAR/\delta Eff$ approaches zero). An initial optimization for the period 1982 to 1984 resulted in 65 percent efficiency (Fig. 4).

The optimized parameters were then used for off-line verification simulations with the observed precipitation data. It should be noted that the optimized parameter set is not unique and represents only one solution set within the optimized parameter space. Figure 5 indicates the results from a multi-year (1985–1988) verification of TOPMODEL at stream gauge 51010 of the Xixian study basin. More than 80 percent of high-flow periods were simulated with both good magnitude and timing. Low-flow periods were within 70 percent of observation. There were a few periods when the observed streamflow went to zero and the simulated result carried a small but significant base flow. There were also questionable observations that may have skewed the efficiency. This is apparent during periods with observed high precipitation and low streamflow (e.g., timesteps 2040 to 2050). The resulting calibrated and verified parameter set (Table 4) has been implemented into the RCSM for hindcast simulation studies at the Xixian study basin.

An interesting diagnostic is the saturated storage deficit (SSD). Figure 6 illustrates the simulated daily variability of the SSD for the Xixian study basin during the year 1982. The SSD is based on a soil moisture mass balance at each timestep. As part of the calibration, SSD was initialized on January 1, 1982 as 40 mm (shallow water table). The SSD increased until day 100 when precipitation exceeded 20 mm/day and again on day 150 when the precipitation exceeded 50 mm/day. Saturation did not occur on day 150 due to the large SSD available. The dry recession periods resulted in increased SSD due to base flow drainage and evapotranspiration. On day 195, a large precipitation event resulted in a SSD less than 5 mm. During the days, 195–210, 225–230, and 232–238 average daily precipitation exceeded 40 mm/day resulting in the SSD becoming negative. Ponding or flooding was simulated to have occurred for days 200–205, 215–220, and 235–245 during 1982. Inter-period near surface saturation may have occurred with periods of high evaporation of ponded water. After these precipitation events, drainage

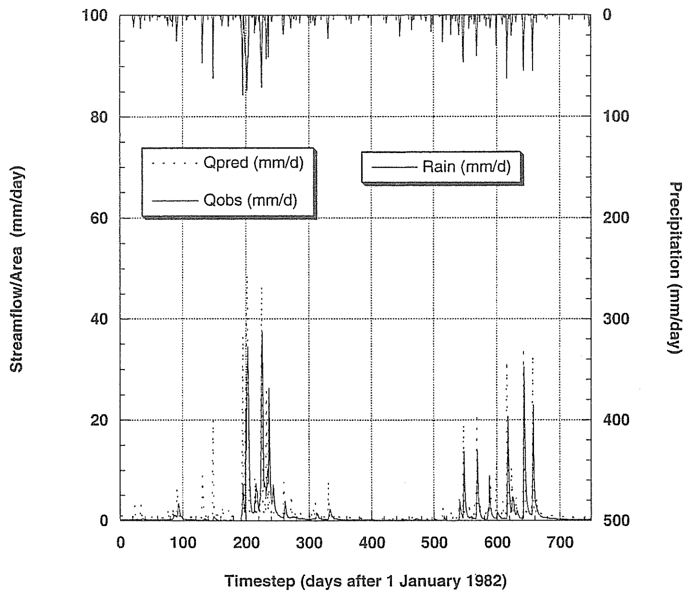

Fig. 4. Results from the TOPMODEL calibration for days 1 to 730.

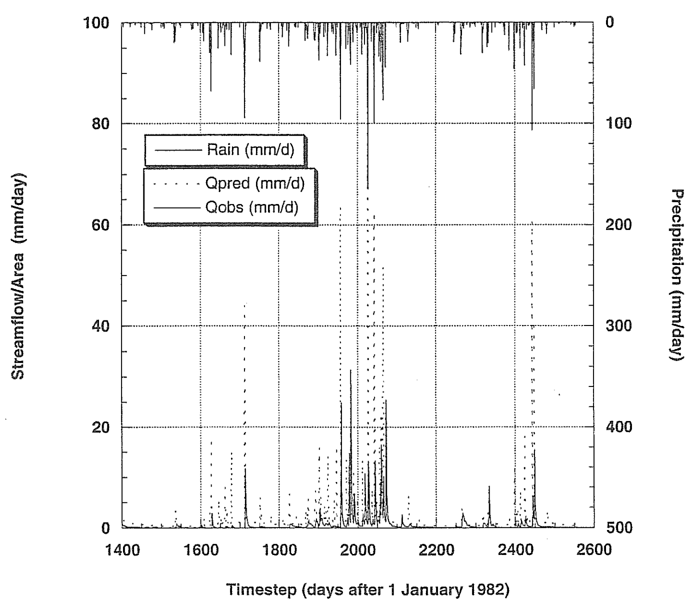

Fig. 5. Results from the TOPMODEL verification for days 1400 to 2550.

Table 4. Calibrated and verified parameter set for TOPMODEL at the Xixian study basin.

Parameter	unit	Description	Value
m	mm	Scaling parameter	60.0
K	mm/day	Saturated hydraulic conductivity	20000.00
1-D	%	Leakage Parameter	5.0
θ	%	Field capacity	35.0
λ_{mean}	ln(m)	Topographic index mean	13.08
$\lambda_{variance}$	$\ln(m^2)$	Topographic index variance	2.02
λ skew	$\ln(m^3)$	Topographic index skewness	1.76
Z_{upper}	m	Soil depth – upper layer	0.45
Z_{total}	m	Soil depth – total	1.20
Z_{root}	m	Root depth	0.40
A	km^2	Total watershed area	2861.00
P_{macro}	%	Percent of precipitation bypassing soil	2.0
P_{imp}	%	Percent of area impervious to infiltration	1.00

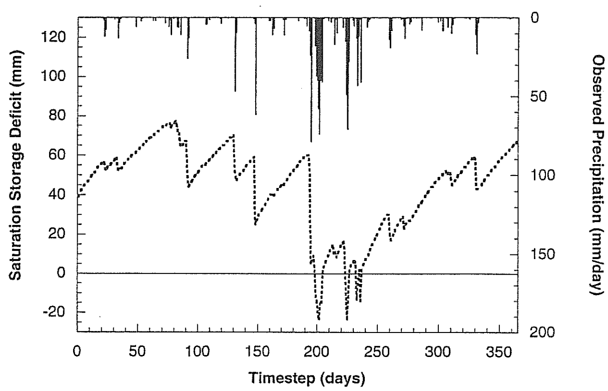

Fig. 6. Results from the TOPMODEL calibration for days 1 to 365. The observed precipitation and simulated saturated storage deficit response during the first year of calibration indicate the periods of saturation.

and evapotranspiration increased the storage deficit to the mid-winter high of approximately 50 mm.

5. Coupled atmosphere-streamflow simulation

A hydroclimate simulation for the period of January 1979 to December 1983 was carried out over the East Asia domain using the RCSM. This long-term climate simulation was initialized with the NCEP–NCAR reanalysis (Kalnay et al. 1996), hereafter Reanalysis, at 00 UTC on January 1, 1979 and continued for five years by prescribing the large-scale forcing with the Reanalysis along the lateral boundaries at 12-hour intervals. A preliminary simulation was made for April 1995 using the same domain and resolution (Kim et al. 1998b). The mean monthly simulated and observed precipitation (Fig. 7) indicates that MAS model can simulate the position and magnitude of the precipitation band with reasonable accuracy, at least qualitatively. Due to the computational limitations at the time of this study all of the simulations were made at the 60 km resolution.

A time series of the simulated and observed mean-monthly precipitation and streamflow for the Xixian study basin is shown in Fig. 8. The precipitation and streamflow trends are well captured, but the JJA and SON seasons, when the heaviest precipitation occurs in this area, are over-predicted by the mesoscale model. Numerical modeling of convective precipitation remains an ongoing topic of research for improvement in climate simulations. The over-predicted precipitation, in turn, results in over-predicted streamflow. The 1983 JJA season resulted with the most accurate simulation, which may be teleconnected or coincidental to the strong 1982 to 1983 El Niño. Scatter diagram comparisons of the observed to simulated precipitation

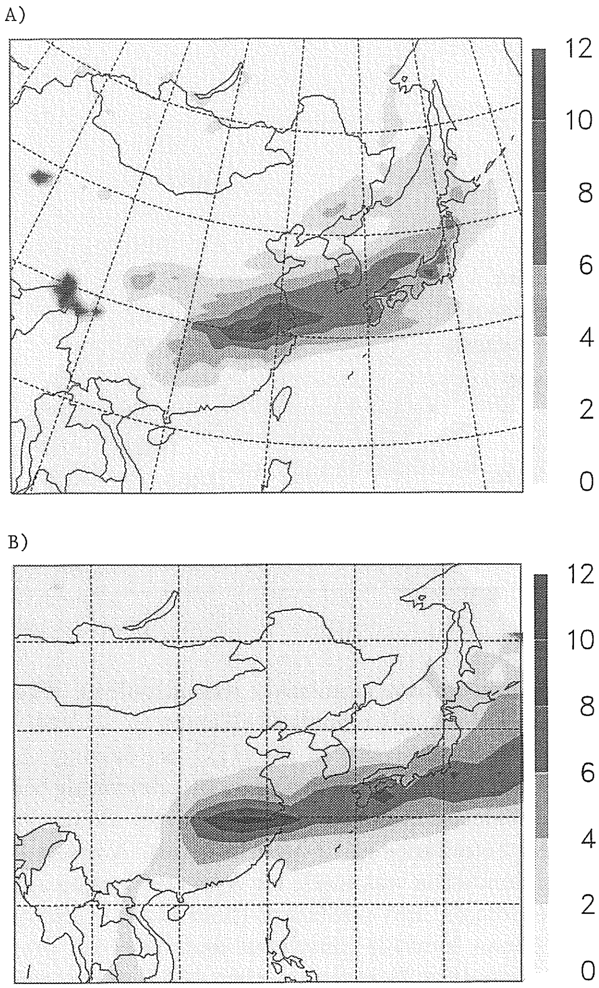

Fig. 7. Monthly mean-daily precipitation (mm/day) for April 1995: a) RCSM-simulated precipitation, b) satellite and rain gauge precipitation data based on the Global Precipitation Climatology Project (GPCP) described in Xie et al. (1998).

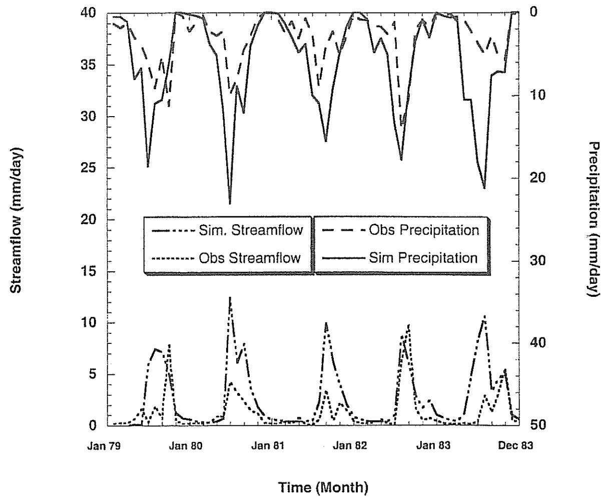

Fig. 8. A comparison of the simulated and observed mean-monthly precipitation and streamflow for the Xixian study basin, January 1979 to December 1983.

and streamflow are shown in Fig. 9. The over-predicted precipitation has a linear correlation of 67 percent and the over-predicted streamflow has a linear correlation of 60 percent. A systematic shift shows up when inspecting these two figures. The cause for increased over-prediction in streamflow is due to a high flow bias that occurs during periods of low precipitation in the simulation. That is, TOPMODEL is calibrated for high flow events and tends to over-predict streamflow during low precipitation periods, where both the observed precipitation and streamflow are low.

The observed and simulated mean-seasonal precipitation and streamflow for Xixian study basin (Fig. 10) indicates that the long-term simulation predicted the DJF, MAM, and SON with fair to good skill. However, during JJA, the over-estimation of precipitation caused the streamflow to be over-estimated. The precipitation bias is −0.4 mm/day, 3.0 mm/day, 8.6 mm/day, and 0.5 mm/day for DJF, MAM, JJA, and SON, respectively. The relative error is 50% for DJF, 120% for MAM, 160% for JJA, and 18% for SON. It can be seen that the trend is good, but the magnitude, particularly during JJA is off. Properly capturing the magnitude and timing of monsoon precipitation is problematic to all atmospheric simulation models. The intense convection that occurs requires further analysis for an improved precipitation scheme. Simulating convection in numerical models is difficult, and an important ongoing research topic (e.g., Hong and Leetma 1999).

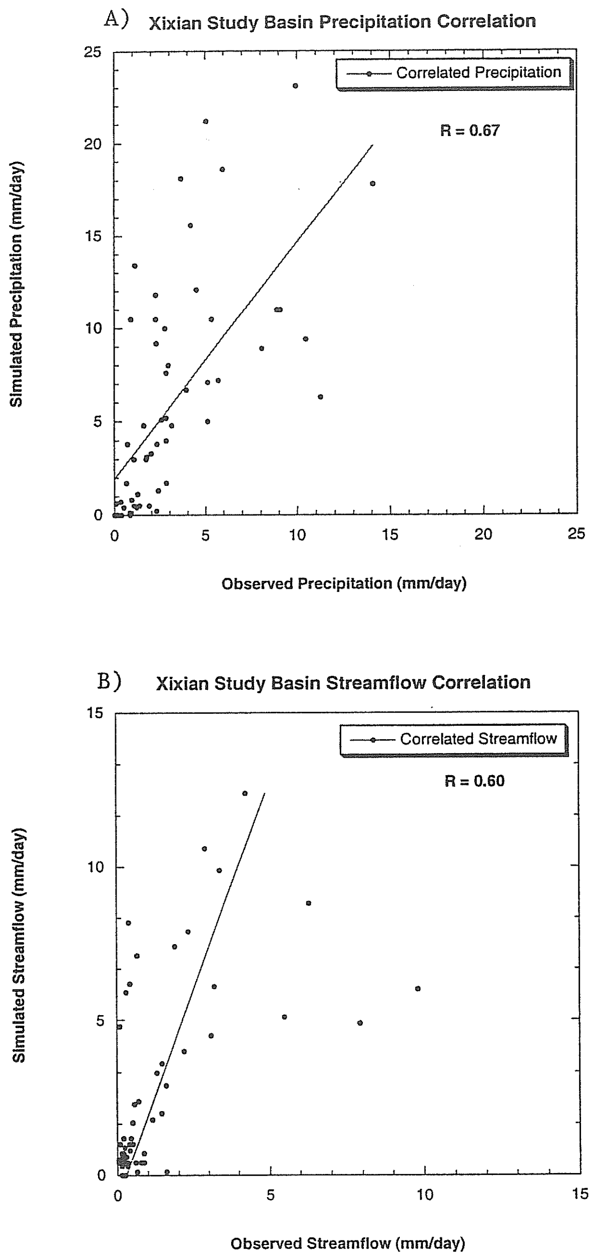

Fig. 9. a) Observed and simulated precipitation correlation plot, and b) Observed and simulated streamflow correlation plot.

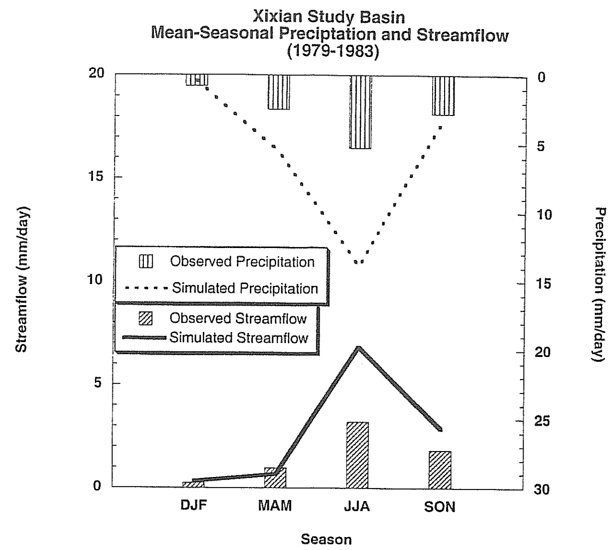

Fig. 10. A comparison of the simulated and observed mean-seasonal precipitation and streamflow for the Xixian study basin based on the seasonal mean values from 1979 to 1983.

6. Discussion

The multi-year simulation indicates the ability of the coupled system to utilize the Reanalysis and simulate mean area precipitation to produce streamflow. This represents a significant first step toward long-term precipitation and streamflow prediction for this region. The mean-monthly analysis indicates a summer time wet season with high streamflow and dry winter and spring seasons with low streamflow. The RCSM-simulated precipitation and streamflow compare well with observations during 1982 and generally over-predicted during other years. The over-prediction was most significant during the summer season, but was close to observations during the fall and winter. The over-prediction may be due in part to the limited quality of the Reanalysis used as large scale forcing in this region, or the mesoscale precipitation scheme.

Several regional climate model simulations for East Asia have indicated similar difficulties producing convective precipitation during the monsoon season (Giorgi et al. 1999; Kato et al. 1999; Wang et al. 2000). Results from Giorgi et al. (1999) and Kato et al. (1999) show that the RegCM gives different precipitation, likely due to different physics used and the different time periods for the simulations. Giorgi et al (1999) used the RegCM to simulate the April and July 1990 precipitation in the eastern Yangtze River basin and over-estimated the observed precipitation by more than 200 percent. Kato et al. (1999) used RegCM to simulate the June 1990 precipitation, and under-estimated the observed precipitation by 50 percent. The May to July 1991 simulation by Wang et al. (2000) using a modified version of the MM5 model reported an over-estimation of summer precipitation in eastern China north of 30°N. The eastern Yangtze River is located at about 31–32°N.

The above results, as well as those in this study, indicate the difficulty in simulating the summer monsoon precipitation in East Asia. Model formulation plays a significant role and the same model (e.g., RegCM) can result in very different results due to differences in the precipitation physics and resolution. In general, atmospheric circulation models show a strong sensitivity to the convection scheme (Kiehl 1992). Giorgi et al. (1999) showed the precipitation physics is very sensitive and Kato et al. (2000) indicated that the effects of spatial resolution will alter the resulting precipitation in RegCM. Additionally, East Asia's unique topography, ocean influence, and large-scale forcing make summertime prediction difficult. The reanalysis, both NCEP and ECMWF, may not be accurate in East Asia due to a lack of observations over the Tibetan Plateau and the Pacific Ocean, as well as possible errors in the assimilation.

Regional climate modeling with streamflow has been applied to regions where most of the heavy precipitation occurs during the winter with little convection with significantly better results. A multi-year hindcast study for the western United States using MAS–SPS at 36 km resolution, and TOPMODEL for a 658 km^2 basin resulted in good precipitation and streamflow skill for a northern California coastal basin (Kim et al. 2000a). This region receives heavy precipitation from January to March, and it is mostly orographically forced precipitation, unlike the convective precipitation during summer monsoons over Xixian. In addition to the type of precipitation, using 36 km resolution for the mesoscale model in this western U.S. simulation has improved both the precipitation and streamflow results. Leavesley et al. (1992) used precipitation from a 90 km resolution regional climate model to a headwater basin in western Colorado with fair to good streamflow results. Leung et al. (1996) used a 90 km resolution regional climate model with an elevation band delineated sub-grid orographic scheme for downscaling precipitation to a small headwater in Montana. This resulted in fair to good streamflow for a river basin west of the continental divide, but indicated an over predicted rain shadow east of the divide. Double nesting of MAS model from 60 km to 12 km will provide improved results that can capture the rain shadow effect. Fine scale precipitation predictions down to 1 km resolution can be simulated by combining the dynamic downscaling with statistical downscaling, depending on the spatial and temporal availability of historical precipitation records.

Further investigation of the observational record, the Reanalysis, and model performance will be required to fully understand this weakness in the simulation. Future improvements will include finer model resolution and more data for evaluation.

7. Conclusions

A coupled atmosphere-streamflow hindcast simulation at the GAME/HUBEX Xixian study basin using the RCSM was performed. Hydrologic model calibration and verification utilized the available land-surface data, and observed precipitation and streamflow records. The multi-year 1979–1983 hindcast simulation indicated that the RCSM can simulate the fall, winter, and spring with fair to good skill. During the summer season, the RCSM has over-predicted the observed precipitation and streamflow. East Asian monsoons remain difficult to simulate due the convection, topography, large scale forcing, and ocean influence. The Regional Climate System Model has indicated the potential for coupled precipitation-streamflow mean-monthly forecasts to improve long-term research and planning for water resources and agriculture in East Asia.

Acknowledgments

We thank Mr. Ryan Eldridge for assisting with land surface and hydrologic data, the Chinese Water Resources Information Center, Ministry of Water Resources for providing data for the Huaihe basin, and the Korean Meteorological Administration, Meteorological Research Institute for generating the Mesoscale Atmopsheric Simulation multi-year climate run for East Asia. This work was supported by the NASA Mission to Planet Earth Program under Grant W19502. The Korean Meteorological Administration, San Diego Supercomputing Center, and the National Energy Research

Supercomputing Center provided computational resources. Work for the U.S. Department of Energy is under contract No. DE–AC–76SF00098.

References

Band, L.E., 1986: Topographic partition of watersheds with digital elevation models, *Water Resources Res.*, **22**, 15–24.

Beven, K.J. and M.J. Kirkby, 1979: A physically-based, variable contributing area model of basin hydrology. *Hydro. Sci. Bull.*, **24**, 43–69.

———, R. Lamb, P.F. Quinn, R. Romanowicz and J. Freer, 1995: TOPMODEL. In Singh (Ed.), Computer Models of Watershed Hydrology. *Water Resources Pub.*, Highland, Colo. 627–668.

Cho, H., M. Niewiadomski and J. Iribarne, 1989: A model of the effect of cumulus clouds on the redistribution and transformation of pollutants. *J. Geophys. Res.*, **94**, 12895–12910.

Deardorff, J.W., 1978: Efficient prediction of ground surface temperature moisture, with inclusion of a layer of vegetation, *J. Geophy. Res.*, **83**, 1889–1903.

Duan, J. and N.L. Miller, 1997: A generalized power function for the subsurface transmissivity profile in TOPMODEL, *Water Resources Res.*, **33**, 2559–2562.

Food and Agriculture Organization (FAO) of the United Nations, 1978: *Soil Map of the World*, scale 1:5,000,000, Vol I-X: U.N. Educat., Scient, and Cult. Org., Paris.

Giorgi, F., Y. Huang, K. Nishizswa and C. Fu, 1999: A seasonal cycle simulation over eastern Asia and its sensitivity to radiative transfer and surface processes. *J. Geophys. Res.*, **104**, 6403–6423.

Hamon, W.R., 1961: Estimating potential evapotranspiration: *Proceed. Amer. Soc. Civil Engrs.*, *J. Hydrau. Div.*, **87**, HY3, 107–120.

Harshvardahn, R. Davies, D. Randall and T. Corsetti, 1987: A fast radiation parameterization for atmospheric circulation models, *J. Geophys. Res.*, **92**, 1009–1016.

Hong, S.-R. and H. Pan, 1998: Convective trigger function for a mass flux cumulus parameterization scheme. *Mon. Wea. Rev.*, **126**, 2599–2620.

——— and A. Leetma, 1999: An evaluation of the NCEP RSM for regional climate modeling. *J. Climate*, **12**, 592–609.

Kalnay, E., M. Kanamitsu, R. Kistler, W. Colins, D. Deaven, L. Gandin, M. Iredell, S. Sara, G. White, J. Woollen, Y. Zhu, M. Chelliah, W. Ebisuzaki, W. Higgens, J, Janowiak, K.C. Mo, C. Ropelewski, J. Wang, A. Leetma, R. Reynolds, R. Jenne and D. Joseph, 1996: The NCEP/NCAR 40-year reanalysis project. *Bull. Amer. Meteor. Soc.*, **77**, 437–471.

Kato, H., H. Hirakuchi and K. Nishizawa, 1999: Performance of NCAR RegCM in the simulation of June and January climates over eastern Asia and the high-resolution effect of the model. *J. Geophys. Res.*, **104**, 6455–6476.

Kiehl, J.T., 1992: Atmospheric circulation model. Chapt. 10, In: (Ed.) K.E. Trenberth, *Climate System Modeling.* Cambridge Univ. Press.

Kim, J., J.-E. Lee and N.L. Miller, 2000a: A multi-year regional climate simulation for the Western United States using the Mesoscale Atmospheric Simulation model. *J. Geophys. Res.*, (In Press).

———, N.L. Miller, J. Farrara and S. Hong, 2000b: A seasonal precipitation study in the Western United States during the 1997/1998 winter season using a dynamic downscaling system. *J. Hydrometeor.*, **1**, 311–329.

———, ———, A. Guetter and K.P. Georgakakos, 1998a: River flow response to precipitation and snow budget in California during the 1994–1995 winter. *J. Climate*, **11**, 2376–2386.

———, ———, J.-H. Oh, J.-Chung and D.-K. Rha, 1998b: Eastern Asian hydrometeorology simulation using the Regional Climate System Model, *Global Planet.* Change. **19**, 225–240.

——— and M. Ek, 1995: A simulation of the surface energy budget and soil water content over the Hydrologic Atmospheric Pilot Experiments—Modelisation du Bilan Hydrique forest site. *J. Geophys. Res.*, **100**, 20845–20854.

——— and S.-T. Soong, 1996: A simulation of a precipitation event in the western U.S. In: Ghan, S., Pennel, W., Peterson, K., Rykiel, E., Scott, M., Vail, L. (Eds), *Regional Impacts of Climate Change.* Battelle Press.

Leavesley, G.H., M.D. Branson and L.E. Hay, 1992: Using coupled atmospheric and hydrologic models to investigate the effects of climate change in mountainous regions: *WRA 28th Ann. Conf. and Symp., Managing water resources during global change.* Reno, Nevada, USA, November 5, 1992, P.691–700.

Leung, L.R., A. Hamlet, D.P. Lettenmaier and A. Kumar, 1999: Simulations of the ENSO hydroclimate signals in the Pacific Northwest Columbia River basin, *Bull. Amer. Meteor. Soc*, **80**, 2313–2329.

———, M.S. Wigmosta, S.J. Ghan, D.J. Epstein and L.W. Vail, 1996: Application of a subgrid orographic precipitation/surface hydrology scheme to a mountain watershed., *J. Geophys. Res.*, **101**, 12803–12817.

Louis, J.F., M. Tieke and J. Gelevyn, 1981: A short history of the Operational PBL-parameterization at ECMWF, *Workshop on Planetary Boundary Parameterization*, 59–79, ECMWF, 260pp.

Marht, L. and H. Pan, 1984: A two layer model of soil hydrology. *Bound. Layer Meteor.*, **29**, 1–20.

Miller, N.L., J. Kim, R.K. Hartman and J. Farrara, 1999: Downscaled climate and streamflow study of the southwestern United States. *J. Amer. Water Resources Assoc.*, **35**, 1525–1537.

——— and ———, 1999: The Regional Climate System Model: Southwestern United States, Eastern Asia, and Northeastern Australia. *WMO/CAS/JSC World Clim. Res. Prog. Rept.*, **No.28**, WMO/TD–No.942.

——— and ———, 1997: The Regional Climate System Model. In: *Mission Earth: Modeling and Simulation for a Sustainable Global System*, (Ed.s) M.G. Clymer and C.R. Mechoso, 55–60.

———, 1997: An Automated Land Analysis System (ALAS) for applications at a range of scales: Watershed to global. In: *Next Generation Environmental Models and Computational Methods*, Chapt.19, (Ed.s) G. Delic and M. Wheeler., Soc. Indust. Appl. Math.

——— and J. Kim, 1996: Numerical prediction of precipitation and river flow over the Russian River watershed during the January 1995 California storms. *Bull. Amer. Meteor. Soc.*, **77**, 101–105.

———, ——— and J. Duan, 1996: The Regional Climate System Model: Southwestern United States and Eastern Asia studies. *WMO/CAS/JSC World Clim. Res. Prog. Rept.*, **No.28**, WMO/TD–No.25., WMO/TD–No.792.

Nash, J.E. and J.V. Sutcliffe, 1970: River flow forecasting throough conceptual models. Part 1: A discussion of principles. *J. Hydro.*, **10**, 282–290.

Pan, H. and W. Wu, 1995: Implementing a mass flux convection parameterization package for the NCEP medium-range forecast model. *NMC Office Note*, 40 pp. NCEP/EMC, Camp Springs, MD, USA.

Starr, D. and S. Cox, 1985: Cirrus clouds. Part I. A cirrus cloud model. *J. Atmos. Sci.*, **42**, 2663–2681.

Stephens, G., 1978: Radiation profiles in extended water clouds. II: Parameterization schemes. *J. Atmos. Sci.*, **35**, 2123–2132.

Soong, S. and J. Kim, 1996: Simulation of a heavy precipitation event in California. *Clim. Chan.*, **32**, 55–77.

Takacs, L. 1985: A two-step scheme for the advection equation with minimized dissipation and dispersion errors. *Mon. Wea. Rev.*, **113**, 1050–1065.

Yu, ZB, Lakhtakia, M.N., Barron, EJ., 1999: Modeling the river-basin response to single-storm events simulated by a mesoscale meteorological model at various resolutions. *J. Geophys. Res.*, **101**, 19675–19689.

Wang, W.-C., W. Gong and H. Wei, 2000: A regional climate model simulation of the 1991 severe precipitation event over the Yangtze-Huai river valley: Part 1. Precipitation and circulation statistics. *J. Climate*, **13**, 74–92.

Xie, PP. and PA. Arkin, 1998: Global monthly precipitation estimates from satellite-observed outgoing longwave radiation., *J. Climate*, **11**, 137–164.